Concerted and Stepwise Reaction Mechanisms for the Addition of Ozone to Acetylene: A Computational Study

Wai-To Chan, Chang'e Weng, and John D. Goddard*

Department of Chemistry, University of Guelph, Guelph, Ontario, Canada N1G 2W1

Received: May 29, 2006; In Final Form: March 16, 2007

The mechanism of the reaction between acetylene and ozone to form a primary ozonide (POZ) in the gas phase has been studied theoretically. The concerted pathway, HCCH + O_3 → POZ, proceeds via a biradicaloid transition state TS0. The stepwise pathway is a three-step reaction, HCCH + O_3 → M1 → M2 → POZ, involving two biradical TSs and two biradical intermediates M1 and M2. The segment of the global potential energy surface (PES) for the concerted pathway is characterized as a R-PES, which is obtained from the restricted (R) density functional theory and Hartree−Fock-based methods. The RDFT and RHF solutions of TS0 and O_3 are unstable toward spin-symmetry breaking. The wave function instability for TS0 and O_3 results in a discontinuity between the R-PES and the region of the global PES encompassing the biradical TSs and the intermediates of the stepwise pathway, which are characterized with unrestricted (U) methods. The global PES is characterized separately as an U(R)-PES using a combination of the R and U methods. Several different values of barriers for the concerted pathway and the energy of concert (E_c) can be estimated due to complications arising from the discontinuity between the R- and the U(R)-PES and the existence of two different RDFT and UDFT O_3 equilibrium geometries. RCCSD(T)//RDFT predicts a barrier of 8.2 kcal/mol. U(R)CCSD(T)/U(R)DFT predicts a barrier of 13.8 kcal/mol for the concerted and 15.3 kcal/mol for the stepwise pathway. Comparison between the R-PES barrier to the concerted pathway and the U(R)-PES barrier to the stepwise pathway suggests the former to be the only significant mechanism. Consideration of the energy difference between TS1, the TS for the first step of the stepwise mechanism, and TS0 within the global PES leads to a significantly smaller E_c. Geometry optimization with CASSCF and energy point calculations with MRMP2 are employed to characterize TS0 and TS1. MRMP2//CASSCF predicts the energy level of TS1 to be higher than that of TS0 by 2 kcal/mol. Analysis of experimental and computational data based on the low estimate of E_c shows that the possibility of the stepwise pathway being a secondary channel at elevated temperatures cannot be ruled out.

1. Introduction

The kinetics and mechanism of the ozonation of acetylene

$$\mathrm{HCCH} + \mathrm{O_3} \rightarrow \text{product}$$

have remained unestablished to this day despite their fundamental importance in the understanding of the role of the cycloaddition of ozone to an alkynic triple bond in atmospheric chemistry. A 1984 review[1] of the gas-phase kinetics of the reactions of ozone documents a series of studies of the reaction beginning from 1953. In the first study,[2] Cadle and Schadt reported a rate constant measured at 303 K. Although higher temperature measurements also were carried out at 313 and 323 K, the Arrhenius parameters derived from these measurements are not accepted as literature values because of the very limited experimental range. In the succeeding study of DeMore[3] dating back to 1969, a parallel study of the ozonation of acetylene and ethylene was carried out. Measurements of the acetylene reaction over the temperature range of 243−283 K yielded an Arrhenius factor ($10^{9.5}$ M^{-1} s^{-1}) higher by 3 orders of magnitude and an activation parameter (10.8 kcal/mol) twice as large relative to the ozonation of ethylene measured over a temperature range of 178−233 K. To explain the large discrepancy between the two *A* factors for the ozonation of ethylene and that of acetylene, DeMore[3] proposed corresponding transition states (TSs) to be of fundamentally different nature, which implicates different reaction mechanisms. Thus, the *A* factor for C_2H_4 + O_3 was determined to be consistent with a five-membered ring TS in a concerted cycloaddition reaction, whereas the much larger *A* factor for HCCH + O_3 would be the result of a stepwise reaction pathway proceeding via an open-chain TS.

Following this work, DeMore[4] reported single-temperature kinetic measurements at 294 K for a series of substituted acetylenes. It was found that variations of the reaction rate constants with the different alkyl groups on the alkynes are relatively small. This behavior sharply contrasts with the more rapid variation observed in the ozonation of substituted alkenes. The conclusion of that study reaffirms the previously measured high *A* factor for acetylene relative to that for ethylene.

Subsequent studies[5,6,7] concern only single-temperature measurements. The absolute rate constants $k(T)$ at or near room temperature (including DeMore's) fall in the range of 0.78−8.6 (in units of 10^{-20} cm^3 $molecule^{-1}$ s^{-1}) over a range of 294−298 K. The lowest value (0.78), as measured by Atkinson and Aschmann at 294 K (see Table 4), is smaller than that of DeMore (1971)[4] measured at the same temperature by a factor

* To whom correspondence should be addressed. E-mail: jgoddard@uoguelph.ca.

10.1021/jp0633188 CCC: $37.00
Published on Web 05/15/2007

of 4 and by 1 order of magnitude from that of Stedman and Niki[5] measured at 298 K. Even taking into consideration the temperature differences, the discrepancies in $k(T)$ are clearly unacceptable if a literature value is to be recommended.

Definitive kinetic data remains unknown to this day. In the 1984 review of Atkinson and Carter,[1] no recommendation of $k(T)$ among the measured values was provided. No measurements have been reported since then, and the current compilations of chemical kinetic data prepared by the NASA Panel for Data Evaluation[8] and by the IUPAC subcommittee on Gas Kinetic Data Evaluation for Atmospheric Chemistry[9] are based on the same literature database as that of the Atkinson review. Instead of taking an average value among available data, the room-temperature rate constant k_{298} is chosen to be unity within the 0.78−8.6 range of experimental data in both compilations. This choice is based on the assumption that the lowest value of Atkinson and Aschmann[7] is the most accurate since one source of uncertainty in the measured $k(T)$ is believed to be the destruction of O_3 in secondary reactions, which could lead to an erroneously high reaction rate. No recommendations of the Arrhenius parameters are provided in the IUPAC compilation. In the NASA compilation, assumed values of the Arrhenius parameters are assigned to fit the recommended k_{298} to the Arrhenius expression $k = A\exp(-E_a/RT)$. The tentatively chosen A factor (1.0×10^{-14} cm^3 molecule^{-1} s^{-1}) is based on the literature value of the A factor for $C_2H_4 + O_3$ (1.2×10^{-14} cm^3 molecule^{-1} s^{-1}) and is of the same order of magnitude as that expected for a five-membered ring cyclic TS for the concerted mechanism according to the analysis of DeMore.[3] The corresponding value of E_a is 8.2 kcal/mol. These assumed parameters are not substitutes for experimental data, and multitemperature measurements are recommended to determine the real Arrhenius parameters.

In a study by Cremer and co-workers,[10a] this uncertainty in the HCCH + O_3 mechanistic pathway was addressed through application of both single- and multireference quantum chemical methods. The activation barrier for the concerted mechanism leading to an acetylene ozonide product (POZ) was predicted with the coupled-cluster method CCSD(T) to be 8.6 kcal/mol, about 2 kcal/mol lower than DeMore's measured value. No biradical intermediates or TSs for the stepwise pathway were found using other methods. DeMore's suggestion of a stepwise mechanism was ruled out in favor of the concerted mechanism. They suggested that DeMore's 1969 measurements were flawed by secondary consumption of the ozone reactants on the grounds that DeMore's measured value of k_{298} is too much larger than their calculated value and the NASA recommended value.[10b] While the CCSD(T) method employed[10a] for the prediction of the concerted mechanism remains the highest level of theory attained, a more thorough characterization of HCCH + O_3 should facilitate further investigations. First, experimental verification of the concerted mechanism must rely on measurement of the A factor over a significant temperature range. However, no appropriate theoretical A factor has been reported.[10c] Second, the argument against the stepwise mechanism based on the absence of biradicals in theoretical calculations, in particular those employing the complete active space SCF method (CASSCF), is surprising. Biradical intermediates and TSs are ubiquitous in the investigation of pericyclic reaction mechanisms,[11] where applications of both conventional methods including density functional theory (DFT) and CASSCF are well established.[12] Biradical intermediates and TSs also have been reported in the characterizations of the PESs of $C_2H_4 + O_3$[13a] and $C_2H_4 + {}^1O_2$,[14] two similar pericyclic reaction systems. It is also unclear whether the concerted pathway can be predicted to exist with the multireference methods employed to exclude the stepwise pathway as there also were no CASSCF results reported for the concerted pathway TS in ref 10a or in a subsequent study[15] extended to the decomposition of the POZ product.

SCHEME 1

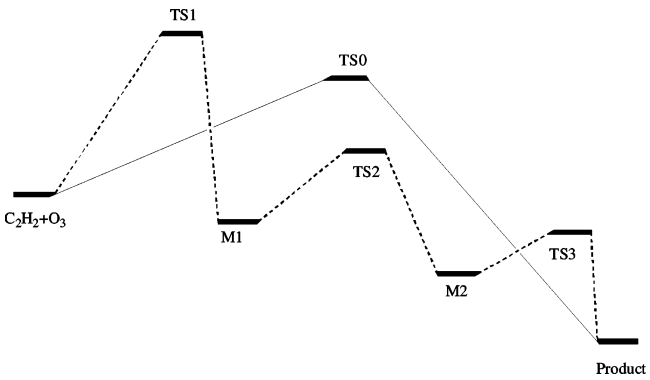

We report a detailed characterization of the PES of HCCH + O_3 using both the restricted (RDFT) and unrestricted density functional theory (UDFT) for geometry optimization of the closed-shell and biradical structures in the PES supplemented by both RHF- and UHF-based CCSD(T) and energy calculations. Contrary to ref 10a, a stepwise reaction pathway is predicted to exist along with the concerted pathway. This stepwise pathway, as depicted in Scheme 1, is the one proceeding via a three-step reaction mechanism involving three TSs (TSn, $n = 1-3$) and two biradical intermediate structures, M1 and M2. The CCSD(T)//DFT prediction of the barrier to the concerted pathway is in close agreement with that of ref 10a. Comparison of the RHF-based CCSD(T) (RCCSD(T)) prediction of the concerted pathway to the UCCSD(T) barrier in the stepwise pathway indicates the former to be the predominant reaction mechanism. CASSCF and the quadratic configuration interaction (QCISD) methods are employed to characterize the key biradical structures to ascertain the existence of both pathways on the PESs. The A factors for the two pathways are reported, and the prospect for the experimental verification of the concerted mechanism based on the predicted data is discussed.

Characterization of a PES encompassing both closed-shell and open-shell singlet structures of varying degrees of biradical character with single-reference methods is complicated by the effects of wave function instability on the continuity of the PES. Some relevant aspects are discussed.

As depicted in Scheme 2, the stepwise pathway and the concerted pathway are placed in one of the R or U regions of the PES according to whether the biradical TS and intermediates are characterized with restricted or unrestricted methods. The concerted pathway is in the R region. The biradical intermediates and TSs in the stepwise pathway are described by U methods because their RHF wave functions (or RDFT solutions) are unstable toward spin-symmetry breaking. Such wave function instability sets in upon distortion of the closed-shell POZ from its equilibrium geometry. As exemplified by the dissociation of the single bond of a closed-shell molecule, the onset of "triplet instability" occurs as the bond is stretched to a point where the closed-shell orbitals become unstable with respect to spin polarization.[16] Beyond this point, the potential energy curve bifurcates into R and U curves associated with RHF/RDFT and UHF/UDFT. Likewise, the energy curve associated with a single-reference-based post-Hartree−Fock method also bifurcates at this point.[17] An UCCSD(T) curve, for instance, would

SCHEME 2

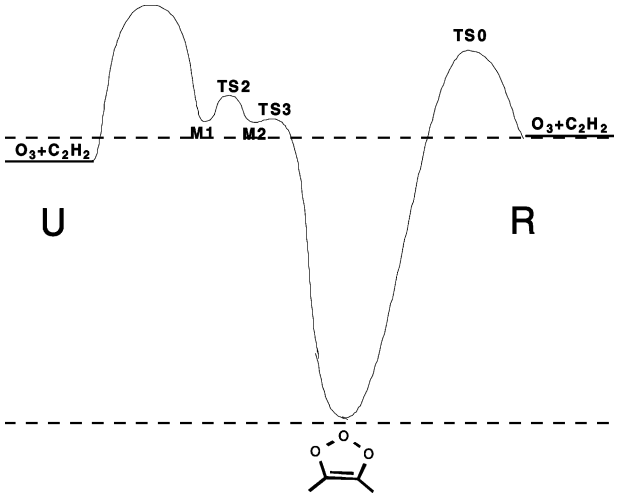

split from the RCCSD(T) curve if two different reference determinants could be used. The two curves represent two separate and thus discontinuous PESs. Hence, an energy difference measured between the two curves beyond the bifurcation point is meaningless.

Discontinuity in a PES of a similar nature is implicated in the global HCCH + O_3 PES. A dilemma faced in the characterization of the R region of the PES is that the RDFT solution of the concerted pathway TS (CTS), TS0, exhibits an instability toward spin-symmetry breaking; a lower energy UDFT solution exists. Nonetheless the RDFT PES is topographically correct in that geometry optimization with RDFT recovers the TS0 structure and predicts the barrier height correctly. The spin-contaminated UDFT PES is distorted from the correct qualitative shape in the vicinity of TS0, and geometry optimization with UDFT fails to predict the geometry of the TS for the concerted pathway. The RDFT solution of O_3, similar to TS0, is also unstable. Unlike TS0, O_3 can be described correctly using either the R or U methods.

Formulation of a precise definition of the energy of concert E_c in light of the wave function instability of the CTS becomes problematic. E_c can be evaluated as the difference between each of the barrier heights to the two pathways from the R and the U region of the PES. This gives a quantity which differs from E_c evaluated as the energy difference between TS0 and TS1 because the reference energy levels of the HCCH + O_3 reactants are different in the two regions. The energy difference between TS0 in the R and TS1 in the U region, however, does not measure E_c on a continuous PES on account of the wave function instability of TS0.

It is not clear if the issue of the influence of wave function instability on E_c has been explicitly addressed. A cursory examination of the literature in the area of theoretical studies of pericyclic reactions[11] indicates that the RDFT- or RHF-based methods such as RMP2 are routinely applied to the characterization of CTSs. Not surprisingly, in the mechanistic study of the ozonation of ethylene and propene,[13a] the CTSs had to be located with RDFT, which is unstable. In a study[18] of the concerted and stepwise pathways of oxygen insertion by dioxiranes into C−H bonds, the concerted pathway from RDFT rather than a stepwise pathway was found to be compatible with experiment. However, these authors held that the precise nature of the CTSs is uncertain due to the instability of the RDFT solutions. Such a view is based on the study by Grafenstein et al.,[19] which stressed the importance of replacing RDFT with UDFT in such situations. Thus, while the primary objective of this study concerns the reaction mechanism of HCCH + O_3, it is also hoped that a comparison of different estimates of using different approaches could contribute to an understanding of this issue.

Following ref 13a, in this study, a single PES, including all of the closed-shell and open-shell structures from the concerted and the stepwise pathways, is predicted by a combination of unrestricted (U) and restricted (R) methods. This PES is termed the U(R)-PES. With the exception of the CTS (TS0), all of the biradical stationary points on the U(R)-PES, including the partial biradical O_3, are located with UDFT. The energies of the stationary points are corrected by application of RCCSD(T) to the closed-shell HCCH and the ozonide product. The UCCSD(T) method is applied to the remaining stationary points, including TS0, which is located by RDFT. The concerted pathway is characterized exclusively with R methods in a R-PES. Both RCCSD(T) and RDFT are employed to characterize the partial biradicals, O_3, and TS0, as well as the closed-shell acetylene and the ozonide product. Thus, the reference energy level used for the evaluation of the reaction barrier to the concerted pathway in this R-PES is different from that for the U(R)-PES. E_c is estimated by taking the energy difference between TS0 and the TS of the first step of the stepwise pathway (TS1) on a single continuous U(R)-PES or between the barrier heights to the two separate pathways on the bifurcated PESs of the R-PES and the part of U(R)-PES covering the stepwise pathway. The different estimates of E_c obtained from CCSD(T)//DFT are compared with the values obtained from multireference calculations on TS0 and TS1.

2. Computational Details

The concerted pathway for the reaction of acetylene with ozone to form a closed-shell primary ozonide (POZ) is

$$\mathrm{HCCH} + \mathrm{O_3} \xrightarrow{\mathrm{TS0}} \mathrm{POZ}$$

where POZ represents the cyclic five-membered ring structure 1,2,3-trioxolene and TS0, the TS structure. The stepwise pathway is a three-step reaction

$$\mathrm{HCCH} + \mathrm{O_3} \xrightarrow{\mathrm{TS1}} \mathrm{M1} \xrightarrow{\mathrm{TS2}} \mathrm{M2} \xrightarrow{\mathrm{TS3}} \mathrm{POZ}$$

where TS (n = 1 to 3), M1, and M2 represent three TSs and two intermediate structures.

The GAUSSIAN98[20] and GAUSSIAN03[21] program packages were employed to perform the DFT, QCISD, and CCSD(T) calculations. BHandHLYP, as implemented in Gaussian with the 6-311+G(d,p) basis set, was used for the geometry optimization and harmonic frequency calculations of the stationary points on the PES. Broken-symmetry DFT solutions and UHF wave functions for the biradical and partial biradical (biradicaloid) structures were obtained using mixing of orbitals to destroy symmetries and through testing of the stabilities of the HF or DFT electronic structures. The equilibrium structure of TS0 was obtained from RDFT. For the geometry of O_3, both RDFT and UDFT were applied. Single-point energy calculations with CCSD(T)/6-311+G(2d,p) were performed on all of the stationary points to construct a R- and an U(R)-PES at the CCSD(T)//DFT level of theory.

To assess the accuracy of DFT and CASSCF and to confirm the existence of the stepwise pathway, the stationary points M1 and M2 were optimized and verified at the QCISD/6-311G(d)

level of theory, and for TS1 and TS2, optimization was at the QCISD/6-311+G(d,p) level of theory.

All of the multireference calculations were carried out using the quantum chemistry program package GAMESS.[22]

Pulay's unrestricted natural orbital-complete active space method (UNO-CAS)[23] was applied to characterize selected biradical structures. This method enables automatic selection of active orbitals for the CASSCF active space based on the fractional occupancies of the natural orbitals (FONO) used as initial guess orbitals as opposed to arbitrary selection of "important" orbitals to design a CASSCF wave function. As originally proposed,[23] the natural orbitals derived from the UHF solution of an even-electron system in the "triplet-unstable" region of the PES provide a good approximation to the CASSCF orbitals and, hence, an appropriate initial guess. Orbitals in the occupancy range of 0.02−1.98 and the total number of electrons contained therein define the CASSCF active space. The fractional occupancies of the UHF-UNO of the initial geometries (obtained from DFT optimization) define an active space of 6 electrons distributed over 6 orbitals denoted as CAS(6,6). CAS(6,6)/6-311G(d) geometry optimizations were carried out. Examination of the FONO of CASSCF of the optimized structures, however, shows the size of the active space to be insufficient. The final geometries and harmonic vibrations were obtained at the CAS(8,8)/6-311G(d) level. For the determination of E_c with CASSCF, only the relative energy levels of TS0 and TS1 are considered. This exclusion of the closed-shell acetylene, nonetheless, avoids the uncertainty in the accuracy of the reaction barriers referenced to the HCCH + O_3 reactants arising from the lack of size consistency of CASSCF.

The CASSCF energies of the optimized structures were corrected through the inclusion of dynamic correlation effects by applying the multireference second-order perturbation theory method (MRMP2), also referred to as the multiconfigurational quasi-degenerate perturbation theory (MCQDPT).[26] Energies of the stationary points were obtained at the MRMP2(8,8)/6-311+G(2d,p)//CAS(8,8)/6-311G(d) level.

High-pressure limiting rate constants for the concerted reaction and the first step of the stepwise pathway are calculated by conventional transition state theory (TST). The rate constants k are evaluated by substitution of the total partition functions of the TS and reactants and the barrier height into

$$k = \frac{k_b T}{h} \frac{Q_{TSn}}{Q_{HCCH} Q_{O3}} \exp(-\Delta E^{\ddagger}/RT)$$

The partition functions are evaluated within the rigid-rotor−harmonic-oscillator approximations using spectroscopic data obtained from the DFT results. The series of k calculated are fit to ln k versus $1/T$ over a temperature range of 243−283 K. The A factor and the Arrhenius barrier E_a are derived from the intercept and slope of this plot to give $k = A\exp(-E_a/RT)$. Higher-level theoretical predictions for the partition functions of TS0 and TS1 also are discussed.

3. Results and Discussion

The geometries of the stationary points on the PESs of the two reaction pathways computed with DFT and, where available, QCISD and CASSCF are given in Figures 1 and 2. The imaginary and the lowest two harmonic frequencies for the TS structures are also included. A tabulation of the electronic and zero-point energies and total entropies is provided in Table 1. Table 2 summarizes the energy levels ($\Delta E/\Delta H_0$) of the TSs and intermediates separately for each of the U(R) and the R-PESs,

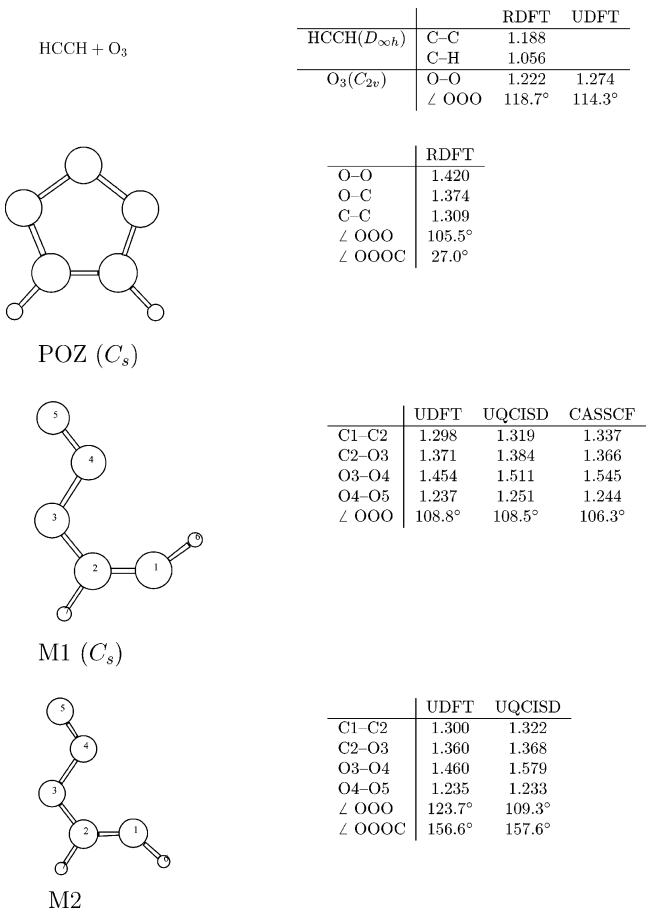

Figure 1. Geometries of reactants, intermediates, and product with bond distances in Å and bond angles in degrees. Dihedral angles of the bond chain C−O−O−O are given for selected structures.

as determined by DFT and CCSD(T)//DFT and for MRMP2//CASSCF. The derived Arrhenius activation barriers (E_a) corresponding to the PES barriers also are included. The FONO data for the CASSCF calculations are collected in Table 3. Table 4 summarizes the experimental and predicted kinetic data. Data required for the evaluation of the partition functions in the TST calculations, molecular mass, harmonic vibrational frequencies, rotational constants, and rotational symmetry numbers, are given in Table 5, which also includes various thermochemical quantities relevant to the discussion of the predicted kinetics. Additional data pertinent to the determination of the Arrhenius parameters are provided in Tables 6−8. Supplementary data including Cartesian coordinates for all optimized stationary point geometries are provided as Supporting Information.

3.1. Concerted Mechanism. The classical barrier $\Delta E^{\ddagger}$ to the concerted reaction via TS0 is 6.8 kcal/mol by RDFT (Table 2). Despite the instability of the RDFT solutions of both TS0 and O_3 toward spin-symmetry breaking, this is in excellent agreement with the RCCSD(T)//RDFT value of 6.7 kcal/mol. Inclusion of zero-point energy places the RDFT barrier (the zero-temperature enthalpy of activation $\Delta H_0^{\ddagger}$) at 8.3 kcal/mol. UDFT frequency calculations at the RDFT geometry of TS0 yield a second imaginary frequency of 151i cm $^{-1}$ (symmetry a″), corresponding to a distortion away from C_s symmetry. Experimenting with an UDFT TS search in the vicinity of TS0 invariably leads to geometries farther from a symmetric structure. Hence, the CTS is concluded to be absent in the DFT U(R)-PES. The concerted pathway barrier obtained from taking the difference between the RDFT energy of TS0 and the U(R)-DFT energy of the reactants gives a value for $\Delta E^{\ddagger}$ of 20.3 kcal/

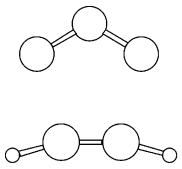

TS0 (C_s)

	RDFT	RQCISD	CASSCF
O–O	1.257	1.293	1.279
O–C	2.123	2.125	2.038
C–C	1.214	1.236	1.256
∠ OOO	112.2°	111.8°	109.8
∠ OOOC	57.1°	57.5	58.2

ω_{1-3}(DFT) = 434i, 247, 276 cm^{-1}
ω_{1-3}(QCISD) = 545i, 234, 262 cm^{-1}
ω_{1-3}(CASSCF) = 827i, 203, 276 cm^{-1}

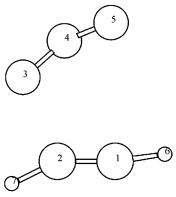

TS1

	UDFT	UQCISD	CASSCF
C1–C2	1.221	1.242	1.252
C2–O3	1.897	1.867	1.846
O3–O4	1.340	1.362	1.396
O4–O5	1.263	1.286	1.245
∠ OOO	112.5°	112.2°	110.9°
∠ H6C1C2	170.1°	167.3°	159.0°
∠ OOOC2	77.3°	71.5°	72.6°

ω_{1-3}(DFT) = 642i, 86, 118 cm^{-1}
ω_{1-3}(QCISD) = 777i, 110, 142 cm^{-1}
ω_{1-3}(CASSCF) = 824i, 104, 151 cm^{-1}

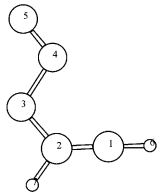

TS2

	UDFT
C1–C2	1.285
C2–O3	1.375
O3–O4	1.454
O4–O5	1.237
∠ OOO	108.9°
∠ H6C1C2	177.7°
∠ OOOC2	25.1°

ω_{1-3}= 608i, 26, 169 cm^{-1}

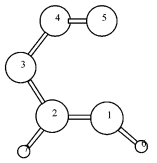

TS3

	UDFT
C1–C2	1.294
C2–O3	1.377
O3–O4	1.425
O4–O5	1.265
∠ OOO	109.7°
∠ H6C1C2	141.6°
∠ OOOC2	53.1°

ω_{1-3}= 247i, 260, 327 cm^{-1}

Figure 2. Geometries and selected harmonic frequencies of transition state structures. The imaginary frequency shown as the first value followed by the two lowest frequencies.

mol, which is three times larger than the corresponding value for the R-PES. This discrepancy apparently arises from the discontinuity between the two PESs. The RDFT geometry of TS0 is in moderate agreement with the CCSD(T)/6-311+G(2d,2p)-optimized geometry reported in ref 10a. Deviations in the O−O, C−C, and the dissociating C−O bond distances from CCSD(T) are 0.015, −0.022, and −0.056 Å, respectively. The larger discrepancy in the O−O distance may be related to the RDFT instability, as a similar difference is also observed in the RDFT O−O distance in O_3, which is 0.058 Å shorter than CCSD(T). UDFT provides more accurate geometries and harmonic vibrations for O_3.[13a] However, the RDFT O−O distance in TS0 is shorter than the UDFT bond distance in O_3, although elongation of the O−O bonds is expected due to the weakening of the bonds in O_3 upon complexation with HCCH. The structural change in O_3 upon proceeding to TS0 is more correctly described by RDFT.

$\Delta E^{\ddagger}/\Delta H_0^{\ddagger}$ from the U(R)-PES (11.5/13.8 kcal/mol) derived from the UCCSD(T)//RDFT energy of TS0 and the UCCSD(T)//UDFT energy of O_3 differs from those of RCCSD(T)//RDFT (6.7/8.2 kcal/mol) and RDFT (6.8/8.3 kcal/mol) from the R-PES by 4 kcal/mol. One source of this deviation is the large discrepancy in the geometry and vibrational frequencies of O_3 between UDFT and RDFT. It is desirable to use the same reactant structures for both the R- and the U(R)-PES. Using the more accurate UDFT geometry of O_3 changes the RCCSD(T) barrier to 10.6/13.0 kcal/mol, reducing the deviations to 1 kcal/mol. Overall, the RCCSD(T)//DFT results of 6.7/8.2 kcal/mol for R-PES are in better agreement with the values of 7.1/8.5 kcal/mol for $\Delta E^{\ddagger}/\Delta H_0^{\ddagger}$ from ref 10a.[10d] The UCCSD(T) barriers are substantially higher.

ΔE for trioxolene formation from CCSD(T) on the R-PES (−61.8 kcal/mol) differs from the U(R)-PES result by 2 kcal/mol. This is due to the energy difference between RCCSD(T)//RDFT and UCCSD(T)//UDFT for O_3. Replacing the RDFT geometry of O_3 with the UDFT geometry changes ΔE to −57.9 kcal/mol for the R-PES, which differs from the U(R)-PES results by 6 kcal/mol. Different energetic estimates thus can be obtained for identical reactions on the two PESs.

3.2. Stepwise Mechanism. The stepwise reaction pathway in the ozonation of acetylene differs from a typical stepwise mechanism for pericyclic reactions and, in particular, from the ozonation of ethylene to form the cyclic ozonide or oxirane described in ref 13a. It is a three-step rather than a two-step reaction. Both ozonation mechanisms share two similar characteristics, that the first reaction is rate-determining and the nearly thermoneutral formation of biradical intermediates.

The first reaction step, similar to that of ethylene and O_3, is essentially the formation of an O−C bond between one end of the alkynic triple bond and one terminal atom of O_3, leading to the adduct M1. The O_3 moiety in TS1 rotates about the C−O bond to an open-chain geometry instead of ring closing. In this rearrangement, the C−H bond at one end flips toward O_3 to assume an "anti" orientation with respect to the other C−H.

$\Delta E^{\ddagger}/\Delta H_0^{\ddagger}$ of the first step is predicted to be 14.8/15.3 kcal/mol by CCSD(T)//DFT. The corresponding values for the concerted pathway are 11.5/13.8 kcal/mol. Hence, for the stepwise pathway, $\Delta E^{\ddagger}$ is predicted to be larger than that for the concerted pathway by 3.3 kcal/mol and $\Delta H_0^{\ddagger}$ by 1.5 kcal/mol for the U(R)-PES. In contrast, the U(R)-PES predicts $\Delta H_0^{\ddagger}$ for the stepwise pathway to be 7.1 kcal/mol higher than that for the concerted pathway predicted by the R-PES. This discrepancy could be partly attributed to the difference in the RDFT and UDFT geometries of O_3. The adjusted barrier (see above) of the R-PES reduces this discrepancy to 2.3 kcal/mol.

In the second step, this C−H rotates away from O_3 such that the two C−H bonds assume a "syn" orientation in M2. This somewhat counterintuitive rearrangement is verified by IRC calculations starting from TS1 and TS2. The final step is a highly facile rearrangement entailing the motion of O_3 in M2 toward the triple bond followed by ring closure to form the product. Geometry optimizations attempting to locate a ring-like intermediate similar to TS3 ends in convergence toward the closed-shell ring structure of the product.

The barrier to the second step is predicted to be 2−3 kcal/mol by both DFT and CCSD(T). Step 3 is a facile reaction with a barrier of 2 kcal/mol at the DFT level and −0.3 kcal/mol at CCSD(T). The precise location of TS3, which occurs in the region of the PES where the energy decreases rapidly due to the change from an open- to a closed-shell electronic structure, must be highly sensitive to the level of theory. Errors in the energies of TS3 and M3 are likely to be a result of a large discrepancy between the CCSD(T) and the DFT PESs in the vicinity of these two stationary points. Precise knowledge of the final step of the stepwise pathway is not likely to be of importance as it is not the rate determining step.

3.3. Concerted Versus Stepwise. E_a corresponding to the various estimates of the $\Delta H_0^{\ddagger}/\Delta E^{\ddagger}$ pair is derived (see Table 2)

TABLE 1: Total Energies and Entropies[a]

	E(DFT)	*S*(DFT)	*E*(QCISD)	*E*(RCCSD(T)	*E*(UCCSD(T))	*E*(CAS(8,8))	*E*(MRMP2)
HCCH	(−77.30168/.0282)	47.46		−77.15460			
O3	−225.35769/.0068	57.04		−225.04953	−225.04618		
	(−225.33617/.0082)	(56.59)		[−225.05571]			
TS0	(−302.62703/.0388)	69.55	(−302.07864/.0363)	−302.19338	−302.18254	−301.29802/.0378	−302.16671
TS1	−302.63843/.0358	74.96	(−302.07526/.0346)		−302.17706	−301.30927/.0351	−302.16385
M1	−302.67164/.0385	76.26	−302.07693/.0371		−302.20361	−301.33048/.0385	−302.17261
TS2	−302.66710/.0367	76.00			−302.19811		
M2	−302.67237/.0384	75.54	−302.07824/.0366		−302.20481		
TS3	−302.66897/.0385	68.41			−302.20519		
POZ	(−302.76233/.0438)	66.61		−302.30265			

[a] The total electronic energies/zero-point energies are in au (electronic energies only for single-point calculations). 6-311+G(d,p) was used for DFT, 6-311G(d) was used for M1 and M2, 6-311+G(d,p) was used for TS0 and TS1 with QCISD, 6-311+G(2d,p) was used for CCSD(T) and MRMP2, and 6-311G(d) was used for CASSCF. RDFT and RQCISD quantities are enclosed in parentheses. UCCSD(T) was performed on the UDFT geometries except for TS0. RCCSD(T) was performed on the RDFT geometries except O_3, for which the RCCSD(T) energy at the UDFT geometry is provided in square brackets. *S*: total entropy ($cal^{-1}\ K^{-1}\ mol^{-1}$).

TABLE 2: Reaction Energies and Barriers of the R- and U(R)-PES[a]

	DFT		CCSD(T)//DFT			CASSCF	
	R	U(R)	R	U(R)	E_a	CAS(8,8)	MRMP2
HCCH + O_3	0	0	0	0	0		
TS0	6.8/8.3	20.3/22.7	6.7/8.2 (10.6/13.0)	11.5/13.8	8.1/13.8 (12.9)	0	0
TS1		13.1/13.7		14.8/15.3	15.8	−7.1/−8.8	1.8/0.1
M1		−7.7/−5.5		−1.8/0.4		−20.4/−20.0	−3.7/−3.3
TS2		−4.9/−3.7		1.7/2.8			
M2		−8.2/−6.0		−2.5/−0.3			
TS3		−6.0/−3.8		−2.8/−0.6			
POZ	−78.1/−73.4	−64.4/−59.1	−61.8/−57.2 (−57.9/−52.4)	−63.9/−58.3			
Expt					10.8 ± 0.4		

[a] Energy levels $\Delta E/\Delta H_0$ (kcal/mol) are referenced to HCCH + O_3 except for those of MRMP2//CASSCF, which are referenced to TS0. ΔE: classical energies; ΔH_0: zero−temperature enthalpies. Energy levels adjusted to the UDFT geometry of O_3 are in parentheses. E_a: Arrhenius activation barriers. E_a for the concerted pathway is associated with TS0 and E_a for the stepwise pathway with TS1. Entries to the left and to the right of "/" correspond to the CCSD(T)//DFT R-PES and the U(R)-PES, respectively. Entry of E_a for TS1 is provided for the U(R)-PES only. The E_a adjusted to the UDFT geometry of O_3 is in parentheses. Expt: experimental barrier as measured by DeMore (1969).

TABLE 3: Fractional Occupancies of UHF and CASSCF Natural Orbitals

	TS0			TS1			M1		
	UHF	CAS(6,6)	CAS(8,8)	UHF	CAS(6,6)	CAS(8,8)	UHF	CAS(6,6)	CAS(8,8)
n_{16}	1.997		1.982	1.996		1.935	1.997		1.982
n_{17}	1.934	1.930	1.931	1.921	1.926	1.928	1.975	1.907	1.914
n_{18}	1.860	1.905	1.906	1.898	1.910	1.910	1.921	1.879	1.880
n_{19}	1.462	1.738	1.742	0.782	1.486	1.489	1.000	1.000	1.000
n_{20}	0.538	0.269	0.266	0.102	0.515	0.512	1.000	1.000	1.000
n_{21}	0.140	0.089	0.086	0.079	0.089	0.089	0.079	0.121	0.120
n_{22}	0.066	0.070	0.068	0.004	0.074	0.073	0.025	0.093	0.085
n_{23}	0.003		0.019	0.003		0.065	0.003		0.019

for DeMore's[3] experimental temperature range of 243−283 K. E_a associated with the CCSD(T)//DFT barrier to the concerted pathway of the R-PES (8.1 kcal/mol) shows the smallest deviation from DeMore's value of 10.8 kcal/mol. E_a for the stepwise pathway (15.8 kcal/mol) derived from the CCSD(T)// DFT U(R)-PES is substantially higher. The R-PES E_a for the concerted pathway referenced to the UDFT structure of O_3 (12.9 kcal/mol) is significantly closer to the U(R)-PES value of 13.8 kcal/mol and the stepwise barrier of 15.8 kcal/mol. On the basis of comparison with ref 10a, the U(R)-PES barrier to the concerted pathway is overestimated, and the most reliable estimate of E_a is 8.1 kcal/mol.

Three estimates of E_c based on the differences between the concerted and stepwise Arrhenius barriers for a specific temperature range can thus be obtained, 7.7, 2.9, and 2.0 kcal/mol. The large variation in the estimates of E_c calls for further determinations of the energy gap between TS0 and TS1.

3.4. Multireference Calculations. The FONOs of the UHF natural orbitals (denoted as the series $n_{17}-n_{22}$) in Table 3 show a range of occupancy within 0.02−1.98 for the three highest formally doubly occupied orbitals and the three lowest formally unoccupied orbitals for TS0 and M1. For TS1, it is the series of occupancies from the 17th to the 21st orbital that falls in the same range, indicating a smaller effect due to correlation. A consistent characterization requires that a single size of active space be used for the entire PES. Hence, all of the three structures are optimized at the CAS(6,6)/6-311G* level. The FONOs of the optimized structures reveal significant deviations between the occupancies of the lowest orbitals in the active space (n_{17}) and of the highest orbitals (n_{22}) from the lower and upper limit of the chosen occupancy range. All three structures are reoptimized at the CAS(8,8)/6-311G* level. One notable change results from increasing the active space size. CAS(6,6)/ 6-311G* yields a single imaginary frequency for the C_s structure

TABLE 4: Summary of Kinetic Data for HCCH + O_3

source	*T*/K	log *A*	E_a	$k(T) \times 1.0e20$
Cadle and Schadt	303			7.8 ± 2.8
	243−283	9.5 ± 0.4	10.8 ± 0.4	
DeMore (1969)	294			4.9*
	303			8.5*
this work		7.3	13.8/8.1/12.9	
(concerted)	243−283			
this work (stepwise)		8.5	15.8	
DeMore (1971)	294 ± 1			3.0
Stedman and Niki	298 ± 2			8.6
Pate et al.	297 ± 2			3.8
Atkinson and Aschmann	294 ± 2			0.78
NASA/IUPAC	298	6.8	8.2	1.0
Cremer et al.	298			0.13

[a] Notes. *k*(T): measured (or recommended) rate constant at temperature *T* (cm^3 $molecule^{-1}$ s^{-1}). *Obtained from extrapolation of the Arrhenius plot. E_a − Arrhenius activation energy (kcal/mol). The *A* factor is in M^{-1} s^{-1}. The *A* factors were calculated at DFT-BHandHLYP for the U(R)-PES. The E_a is at the CCSD(T)//DFT calculated level. Entries of DFT E_as were corrected by CCSD(T) for separate PESs, U(R)-PES/R-PES/adjusted R-PES.

of M1. At the CAS(8,8)/6-311G* level, the C_s structure is a genuine minimum. Examination of the resulting CAS(8,8) FONO shows similar deviations between the occupancies of the lowest and highest orbitals in the (8,8) active space size from 0.02 and 1.98 for TS1. The FONOs in the active spaces of TS0 and M1, however, fit very closely into the 0.02−1.98 range. Extension to CAS(10,10) is prohibited by the costly TS optimization. The final geometries are reported at the CAS(8,8) level.

Comparison between the DFT and CASSCF geometries of TS0, TS1, and M1 shows the two methods to be in overall qualitative agreement for structures. Both methods recover the TS for the concerted pathways and predict a geometry for M1 with C_s symmetry. The largest discrepancy is found in the O−O bond adjacent to the C−O bond linking the O_3 moiety to HCCH, where CASSCF predicts a bond distance that is 0.1 Å longer than that from DFT for M1. QCISD predicts a value intermediate between the two methods. For TS0, CASSCF predicts bond distances in the O_3 group in better agreement with RQCISD than RDFT. This may be a result of the instability of the RDFT solution. Substantial discrepancies are also observed in the imaginary vibrations of TS0 and TS1. CASSCF predicts a rather similar imaginary frequency for each of two TSs which are nearly 400 cm^{-1} larger for TS0 and 200 cm^{-1} larger for TS1 than that from DFT.

The energies predicted by CASSCF for TS1 and M1 relative to TS0 as shown in Table 2 differ significantly from all of the other estimates. TS1 is placed at a level that is about 8 kcal/mol lower than TS0. M1, which is predicted to be thermoneutral by CCSD(T), is placed at 20 kcal/mol below TS0. Thus, CASSCF predicts the stepwise pathway to be the only significant mechanism with an unusually high stability of the first biradical intermediate formed.

The apparently anomalous CASSCF results are not entirely surprising. The size of the active space adopted amounts to only a fraction of the size of a full-valence CASSCF treatment required for a balanced characterization of the global PES. It is understood that CASSCF recovers only a modest amount of correlation energy that is usually considered to be the "static" portion of the total correlation energy. In fact for pericyclic reactions and other multireference systems, the absence of dynamic correlation energy in CASSCF can lead to qualitatively incorrect results.[24] Hence, the accuracies of the predicted geometries and energetics of CASSCF are not necessarily greater than those from DFT. One feature that distinguishes CASSCF from DFT is that the biradical character of TS0, along with other structures, is explicitly described in its wave function. The biradical character index[25] of TS0, as measured by $(2 - n) \times 100\%$ (with *n* being the occupancy of the highest occupied orbital), shows TS0 and TS1 to be partial biradicals with 26 and 51% biradical character, respectively. M1 is a pure biradical. In contrast, within the single-reference formalism, TS0 is absent in the UDFT PES and has to be treated as a closed-shell system for structural optimization. The steep decrease in energies concomitant with the increase in the biradical characters of these species suggests that CASSCF may overestimate the stability of biradicals and, hence, incorrectly favors the stepwise mechanism.

Quantitative accuracy cannot be expected of CASSCF. A sufficient amount of static correlation energy may have been captured in the CASSCF wave function to enable qualitative prediction of the biradical PES. Thus, it is reasonable to expect that using the CASSCF wave functions as the zeroth-order wave functions in the MRMP2 method could yield a qualitatively correct and quantitatively more reliable representation of the biradical PES through the concerted and stepwise pathway TSs.

From Table 2, the CASSCF energy of TS1 relative to TS0 is changed from −7.1 to 1.8 kcal/mol by MRMP2/6-311+G(2d,p). Inclusion of the CASSCF zero-point energy narrows this gap to only 0.1 kcal/mol. The energy level of M1 is corrected to a value of −3.7/−3.1 kcal/mol. This estimate of the energy of M1 remains problematic. The energy gap between M1 and TS0 is estimated to be as large as 13−14 kcal/mol by CCSD(T). For M1 to be thermoneutral, the MRMP2 barrier to the concerted pathway has to be less than 4 kcal/mol, which is one-half of the lowest estimate by CCSD(T)//DFT. Further investigation reveals the presence of a high-lying state within a fraction of 0.0001 au above the ground state of M1. High-lying states that are quasi-degenerate with the ground state are known to cause singularities in the MRMP2 PES.[27] Preliminary CASSCF excited-state calculations also show a larger gap of 0.0003 au between the first excited state and the ground state of M2. For TS0 and TS1, this energy gap is found to be as large as 0.03−0.1 au, and the influence of high-lying states can be ruled out. It is possible that the small singlet−triplet gap in pure biradicals could cause difficulties for the construction of a continuous MRMP2 PES extended from the partial biradicals TS0 and TS1 to the biradical intermediates.

The MRMP2 value of E_c is in close agreement with the smallest value obtained from CCSD(T)//DFT. The value of E_c of 2.0 kcal/mol obtained by taking the difference of E_a of the two pathways derived for the U(R)-PES is more comparable to the MRMP2 value in that the energies of TS0 and TS1 in both derivations are determined at the same level of theory. In the calculation of the largest estimate (7.7 kcal/mol), TS0 is predicted with RCCSD(T) based on an unstable wave function and TS1 with UCCSD(T), and the two TSs are referenced to a different reactant energy. To further illustrate the dependence of the high estimate of E_c on the reference energy, the tabulated energetic data is shown in Table 1. Taking the difference between the RCCSD(T) energy of TS0 and the UCCSD(T) energy of TS1 gives a value of 10.2 kcal/mol. This value can be compared with the difference between the corresponding values $\Delta E^{\ddagger}$ in Table 2, which give an estimate of 8.1 kcal/mol. The low estimate for E_c could be a consequence of an overestimation of the barrier to the concerted pathway by UCCSD(T), narrowing the gap between TS0 and TS1. However, if E_c is defined as the energy difference between TS0 and TS1 within a single continuous PES, it would be the low estimates of UCCSD(T) and MRMP2 that satisfy this definition. The

TABLE 5: Data for Molecular Partition Functions[a]

temp (K)		HCCH	O_3	TS0	TS1
	molecular mass (amu)	26.01565	47.98474	74.00039	74.00039
	σ	2	2	1	1
	rotational constant	RDFT	UDFT	RDFT/RQCI	UDFT/UQCI
	(cm^{-1})A_e	1.21	3.32	.322/.308	.345/.323
	B_e		.459	.189/.188	.145/.154
	C_e		.404	.125/.123	.108/.113
298	Q_{rot}	85.8	3.38e04	6.06e04/6.30e05	7.22e05/7.14e05
〃	S_{rot} (cal/mol/K)	10.8	19.1	24.9/24.9	25.2/25.2
	vibrations	ω	ω	$\omega/\omega_{qci}/\nu$	$\omega/\omega_{qci}/\nu$
	(cm^{-1})	735	727	433i/546i/464i	642i/765i/674i
		735	1107	247/229/240	86/111/62
		817	1158	276/260/267	118/135/117
		817		450/415/445	278/293/268
		2139		507/495/464	396/381/406
		3504		766/660/743	598/564/598
		3612		789/711/774	689/654/674
				793/743/777	736/687/720
				810/762/802	801/778/785
				829/787/816	880/808/868
				1225/1059/1207	996/966/971
				1281/1063/1253	1250/1092/1219
				1978/1855/1953	1892/1819/1868
				3491/3419/3373	3456/3385/3338
				3576/3496/3452	3545/3474/3416
298	Q_{vib}	1.102/1.196	1.040/1.041	2.698/3.185/2.832	12.81/9.52/17.41
	S_{vib}				
283	(cal/mol/K)			5.37/6.18/5.59	10.36/9.72/11.17
298		0.92/1.46	0.39/0.41	5.86/6.72/6.09	10.84/10.32/11.76
323				6.68/7.63/6.92	11.90/11.31/12.74

[a] Notes. σ: rotational symmetry number. Q_{rot}, Q_{vib}: total rotational and vibrational partition functions. S_{rot}, S_{vib}: total rotational and vibrational entropies. ω, ω_{qci}, ν: DFT harmonic, QCISD harmonic, and DFT fundamental vibrations.

TABLE 6: Summary of Data for the Derivation of Arrhenius Parameters[a]

	concerted					stepwise				
T/K	log A_{bot}	$\Delta E^{\ddagger}$	log A_0	$\Delta H^{\ddagger}$	$k(T)$	log A_{bot}	$\Delta E^{\ddagger}$	log A_0	$\Delta H^{\ddagger}$	$k(T)$
243	8.316	20.29	10.46	21.54	.116E−09	10.65	13.14	11.12	13.02	.0680
251	8.380	20.29	10.45	21.52	.514E−09	10.67	13.14	11.13	13.02	.171
259	8.440	20.29	10.45	21.51	.208E−08	10.70	13.14	11.14	13.02	.408
267	8.497	20.29	10.45	21.50	.771E−08	10.72	13.14	11.15	13.02	.926
275	8.551	20.29	10.44	21.48	.255E−07	10.74	13.14	11.16	13.02	2.01
283	8.602	20.29	10.44	21.47	.855E−07	10.76	13.14	11.17	13.03	4.17
298	8.693	20.29	10.44	21.45	.647E−06	10.81	13.14	11.19	13.03	14.8
E_{cor}			−8.8		−8.8			1.7		1.7

[a] All kinetic and energetic quantities were derived from the DFT U(R)-PES. Energies are in kcal/mol. The A factors and $k(T)$ are in $cm^3\ mol^{-1}\ s^{-1}$. $\Delta E^{\ddagger}$: classical barrier. $\Delta H^{\ddagger}$: enthalpy of activation. The A factor is referenced to the zero-point vibrational level denoted as A_0, referenced to the bottom of the potential surface denoted as A_{bot}; $k(T) = A_{bot}\exp(-\Delta E^{\ddagger}/RT) = A_0\exp(-\Delta H^{\ddagger}/RT)$. E_{cor}: energy correction to correct DFT barriers based on the CCSD(T)//DFT U(R)-PES (see Table 2).

TABLE 7: Molecular Partition Functions of HCCH and O_3[a]

	HCCH				O_3			
T/K	Q_{trans}	Q_{rot}	Q_{vi}(bot)	$Q_{vib}(0)$	Q_{trans}	Q_{rot}	Q_{vib}(bot)	$Q_{vib}(0)$
243	.9456E32	70.00	.1334E−15	1.043	.2369E33	2485.	.1447E−3	1.016
251	.9927E32	72.30	.4310E−15	1.050	.2487E33	2608.	.1924E−3	1.019
259	.1041E33	74.61	.1297E−14	1.057	.2607E33	2734.	.2515E−3	1.022
267	.1089E33	76.91	.3655E−14	1.065	.2728E33	2862.	.3235E−3	1.025
275	.1138E33	79.21	.9710E−14	1.074	.2852E33	2991.	.4104E−3	1.028
283	.1188E33	81.52	.2443E−13	1.083	.2977E33	3123.	.5139E-3	1.032
298	.1284E33	85.84	.1209E−12	1.102	.3217E33	3374.	.7591E−3	1.040

[a] Q_{trans}: translational partition function (m^{-3}). Q_{rot}: rotational partition function. $Q_{vib}(0)$, Q_{vib}(bot): vibrational partition function relative to the zero-point energy level and to the bottom of the potential surface, respectively.

MRMP2//CASSCF data as a representation of a continuous PES through TS0 and TS1 do not suffer from the effects of spin contamination and wave function instability. The close agreement between MRMP2 and UCCSD(T) supports the view that the U(R)-PES data closely approximates a single continuous PES. This view implicitly assumes that there exists a TS0 in the UCCSD(T) PES. It is observed that UDFT suffers from spatial-symmetry breaking at the geometry of TS0. In other calculations, TS0 is located with RQCISD in this study and with RCCSD(T) in ref 10a. Whether TS0 coexists on both an UHF-based and a RHF-based PES is uncertain. The modest correlation in MRMP2 relative to CCSD(T), however, also

TABLE 8: Molecular Partition Functions of TS0 and TS1[a]

	TS0				TS1			
T/K	Q_{trans}	Q_{rot}	Q_{vib}(bot)	$Q_{vib}(0)$	Q_{trans}	Q_{rot}	Q_{vib}(bot)	$Q_{vib}(0)$
243	.4537E33	.4463E5	.2521E-21	1.916	.4537E33	.5311E5	.4545E-19	7.410
251	.4762E33	.4685E5	.1316E-20	2.009	.4762E33	.5575E5	.2170E-18	8.025
259	.4992E33	.4911E5	.6232E-20	2.108	.4992E33	.5844E5	.9451E-18	8.691
267	.5225E33	.5140E5	.2698E-19	2.213	.5225E33	.6117E5	.3787E-17	9.412
275	.5462E33	.5373E5	.1076E-18	2.327	.5462E33	.6394E5	.1406E-16	10.19
283	.5702E33	.5609E5	.3987E-18	2.448	.5702E33	.6675E5	.4869E-16	11.04
298	.6161E33	.6060E5	.3877E-17	2.698	.6161E33	.7212E5	.4223E-15	12.81

[a] See footnote for Table 7.

means that accuracy of the low estimate of E_c is subject to uncertainty. It thus seems prudent to consider the different experimental implications of both the high and low estimates.

3.5. Kinetics. On the basis of comparison with experimental data, the procedure employed in this study was shown earlier[13a] to be accurate to within 1 order of magnitude for the prediction of the *A* factor for the concerted mechanism in the ozonation of ethylene and propene.[13b] Provided that the real *A* factors for the concerted and the stepwise pathway are sufficiently different, the accuracy of the estimated *A* factor for the concerted pathway for HCCH + O_3 is expected to be adequate.

From Table 4, the measured *A* factor for acetylene ozonation by DeMore[3] is $10^{9.5}$ M^{-1} s^{-1} (log $A = 9.5$). The DFT value of log *A* obtained for the concerted pathway is 7.3. The DFT value for the first step of the stepwise pathway is 8.5. Thus, DeMore's *A* factor is greater than the theoretical *A* factor for the pathway predicted to be the thermochemically favored mechanism by 2 orders of magnitude. Discrepancies of such magnitude suggest either experiment or theory (or both) fail. DeMore's *A* factor can be accounted for by neither a CTS nor a stepwise TS. Analysis in ref 10a suggests that DeMore's rate constant is too large to be correct. If the conclusion in ref 10a is accepted, this report could be ended and the present estimate of the concerted *A* factor recommended for future kinetic measurements. Further examination of the experimental data is warranted when theory contradicts experiments.

The kinetics of HCCH + O_3, which are measured in terms of the decay rate of O_3 could be effected by secondary reactions between O_3 and the radical intermediates. This is cited by Cremer et al.[10a] to explain the discrepancy between their calculated rate constant and DeMore's data. Examination of the kinetic data tabulated in Table 4 shows that the k_{298} of ref 10a (0.13) is 1/6 of the lower limit and less than 1/10 of the upper limit of the range of experimental data. Acceptance of this value implies that none of the known experimental rate constants are reliable. An a priori knowledge of kinetics only can be obtained from experiments. Theory can provide qualitatively correct *A* factors for key reaction steps to aid experimental identification of the mechanism. It is first assumed that the true reaction rate falls into the range of the available data. The reliability of DeMore's Arrhenius plot for the 243−283 K range is assessed based on this assumption.

In DeMore's 1971 study,[4] the value of $k(T)$ measured at 294 K (see Table 4) and the value of Cadle and Schadt[2] at 303 K were compared with the original 1969 Arrhenius plot.[3] The $k(T)$s obtained from extrapolations of the original Arrhenius plot are in close agreement with these two directly measured values within the error ranges of the Arrhenius parameters (see Table 4). The good agreement between three independent measurements led DeMore to consider surface reaction as a possible source of serious errors to be unlikely. Signs of secondary consumption of O_3 by radicals produced in the reaction were observed. Upon addition of O_2 as a radical scavenger, the decay rate of O_3 was reduced substantially until higher O_2 concentration produced no further effect. The reaction was determined to be stoichiometric based on the consumption ratio of O_3. Hence, DeMore concluded that the surprisingly high *A* factor from 1969 was correct. This conclusion, however, was reached before the other known values of $k(T)$ were reported. The largest value of $k(T)$[5] of 8.6 at 298 K is greater than DeMore's $k(T)$ at 294 K by a factor of 3. More discomfiting is that the $k(T)$ of Cadle and Schadt at 303 K is smaller than this value measured at a lower temperature. If the lowest measured value of Atkinson and Aschmann,[7] on which the literature value is based, is referred to as the lower bound of the true $k(T)$, DeMore's $k(T)$ would be more reliable than others. However, this assumption still gives an estimated maximum error of 75% in DeMore's $k(T)$. The corresponding errors in DeMore's Arrhenius parameters are relatively modest but fall outside of their range of uncertainties (see Table 4). Thus, reducing log *A* from 9.5 to 8.7 or increasing E_a from 10.8 to 11.9 kcal/mol would give an extrapolated value of $k(T)$ at 294 K in agreement with the value of Atkinson and Aschmann.

Applying the corrections above, however, cannot account for the two-order-of-magnitude deviation between the calculated *A* factor for the concerted pathway and the measured value. A corrected *A* factor intermediate between DeMore's and the predicted value would contradict a conclusion that the concerted pathway is the favored mechanism. If the real energy of concert is closer to the low limit of the estimates given earlier, the stepwise mechanism could play a role as a secondary channel. Experimental indications of such a parallel-pathway mechanism was not observed. Comparison between DeMore's extrapolated Arrhenius plot[3] and the two measurements of $k(T)$ at 313 and 323 K of Cadle and Schadt[2] revealed a large discrepancy, although the Arrhenius plot of Cadle and Schadt was in close agreement with DeMore's in the temperature range of 298−303 K. This discrepancy was observed by DeMore[3] but was never further addressed. Taking this discrepancy as a possible experimental indication of non-Arrhenius kinetics, the influence of the stepwise pathway is tested below.

Taking the ratio of the two Arrhenius expressions corresponding to the two competing pathways based on the E_c of 2 kcal/mol derived from the U(R)-PES gives $13.8\exp(-1005.5/T)$ for the ratio k_s/k_c, with k_c being the rate constant for the concerted pathway. The crossing-point temperature at which this ratio is unity is about 383 K. This ratio increases from 0.22 at $T = 243$ K, the lowest temperature of the experimental range studied by DeMore,[3] to 0.47 at 323 K, the upper limit of the range of Cadle and Schadt.[2] Thus, the stepwise pathway is a significant secondary channel at elevated temperatures. The contribution of the stepwise reaction to the overall kinetics increases with temperature because of the entropic advantage of TS1 over TS0, as reflected in the relative sizes of their *A* factors. The total entropy at room temperature of TS1 (Table 1) is larger than that of TS0 by 5 eu. This entropic difference would be sufficient to offset a small energy difference between the two TSs on the PES.

The above analysis raises the possibility that the HCCH + O_3 reaction proceeds by two parallel reactions involving the concerted pathway as the dominant channel at low temperatures and, upon increasing temperature, the stepwise channel as a minor secondary channel. A theoretical analysis[29] has shown deviation of the Arrhenius plot for a model of parallel reaction mechanisms from either of the two Arrhenius plots derived separately. Such may explain DeMore's observation of an *A* factor which is unexpectedly high for the reaction to proceed exclusively by a concerted mechanism.

The stepwise pathway would be a competing channel if the low estimate of E_c was accurate and was not effected by the overestimation of the concerted barrier by UCCSD(T) relative to that of RCCSD(T). It can be seen that the energy levels of the HCCH + O_3 reactants embedded in k_s/k_c are eliminated since there is only a reference energy level for both reaction pathways in the U(R)-PES. Hence, the ratio is dependent on E_c as the energy difference of TS0 and TS1 and independent of the reaction barriers. Caution is, however, warranted in considering the possible significance of the stepwise channel on account of the sensitivity of the reaction rate to the energy barrier. A modest error in E_c could translate to a significantly smaller k_s/k_c. Another significant error in E_c, the entropic difference between TS0 and TS1 at elevated temperatures, can also affect the extent of the role of the secondary channel. Treatment of a hindered-internal-rotor mode as a harmonic oscillator and neglect of anharmonicity are sources of errors in the entropies of the low-frequency vibrations which contribute most to the total vibrational partition functions.

The harmonic vibrations of HCCH, O_3, TS0, and TS1 and thermodynamic quantities including rotational and vibrational entropies used as input to the TST calculations are tabulated in Table 5. Visualization of the lowest five real harmonic frequencies of TS1 shows that the first four modes resemble ring puckering motion. The fifth mode (598 cm^{-1}) is the bending motion of one of the HCC angles. No internal rotation around any one of the bond axes can be identified. Ayala and Schlegel's procedure[30] of automatic identification of internal rotation does not identify any vibration that requires correction. The reason for the absence of internal rotation is that the geometry of TS1 is closer to a partial ring structure than a linear chain. The bond length of the partial C−O bond (2.918 Å) is longer than the C−O bond in TS0 by 0.9 Å, but presumably, the geometry is still compact enough to inhibit internal rotation around one single bond in the ring skeleton. Not unexpected is that internal rotations also are not identified in TS0, but for M1, which assumes an open-chain geometry, three modes are identified as internal rotations, including the two smallest vibrations. Treatment of these modes as internal rotation instead of normal modes leads to a correction of −0.121 cal/mol/K to the total vibrational entropy.

Comparison between the QCISD and DFT harmonic frequencies reveals generally good agreement in the low frequencies of TS0 and TS1. QCISD gives slightly higher frequencies for the first two vibrations of TS1. Such small shifts result in considerable discrepancies in the total vibrational entropies, which are highly sensitive to changes in the small frequencies. The QCISD entropic difference between TS1 and TS0 at room temperature (3.6 eu) is smaller than the DFT value of 5 eu. At 323 K, the DFT value is still about 1.5 eu larger. At temperatures above 300 K, this smaller entropic advantage of TS1 relative to TS0 is still sufficiently large for the stepwise pathway to be significant for a E_c within 2 kcal/mol.

Anharmonic frequencies (fundamental bands) of TS0 and TS1 are calculated with a procedure based on numerical differencing of analytic second-order derivatives to obtain higher-order derivatives[31] implemented in GAUSSIAN03. Vibrational entropies are evaluated by replacing harmonic frequencies with the anharmonic values in the standard expression of the harmonic oscillator partition function.[32] Although DFT is likely to be less accurate than high-level methods such as QCISD, in general, DFT predictions of vibrational anharmonicities have been shown to be reliable.[33] The purpose here is to determine in what direction a correction for anharmonicity would change the entropic advantage of TS1.

In common with experience in empirical scaling of harmonic frequencies to correct for anharmonic effects, the calculated fundamental frequencies are all smaller than their harmonic counterparts. The lowest frequency of TS1 is adjusted from 86 to 62 cm^{-1}. This change effects a slight increase in the entropic difference with TS0 from 4.98 to 5.67 eu at 298 K. This amounts to a modest increase of the entropic advantage of TS1 from the use of DFT harmonic frequencies by 0.7 eu. At 323 K, this increase becomes 0.6 eu. This increase is smaller than the decrease in entropic difference between the two TSs resulting from the use of QCISD harmonic frequencies.

Thus more accurate estimates of the entropic difference between TS1 and TS0 do not qualitatively affect the prediction of the stepwise pathway as a minor secondary channel at elevated temperatures.

3.6. Recommendations for Further Experimental Investigations. The concerted pathway is predicted to be favored. However, the moderate agreement between DeMore's rate constants and the literature value suggests the possibility that the error in DeMore's *A* factor could be smaller than a two-order-of-magnitude deviation from the theoretical *A* factor for the concerted mechanism. In light of this possibility, the present estimates of the Arrhenius parameters should be viewed as an aid to future experiments rather than as a definitive mechanistic prediction.

Comparison and analysis of experimental and theoretical data are based on the assumption that the true value of the room-temperature rate constant approaches the literature value between the measured values of DeMore[3] and of Atkinson and Aschmann.[7] Discrepancy between these two values is smaller than the maximum uncertainty of available experimental data. It is recommended that accurate measurements aimed to establish the quantitative accuracy of the room-temperature rate constants to within a smaller uncertainty could greatly facilitate the multitemperature measurements as recommended in the NASA compilation.

It is suggested that verification of a concerted mechanism for acetylene ozonation can be realized through an extension of DeMore's 1969 measurements to a higher and broader temperature range through the upper limit of Cadle and Schadt's study[2] (323 K) and beyond. Observation of Arrhenius kinetic behavior similar to that of ethylene ozonation would establish the mechanism of acetylene ozonation to be a concerted one-step reaction. A linear Arrhenius plot with an *A* factor larger than the predicted value for the concerted pathway by more than 1 order of magnitude could indicate that the stepwise mechanism is predominant. This possibility is considered unlikely, for the true E_c has to fall outside of its estimated range. Significant deviation from Arrhenius kinetics, as evidenced by a curvature in the Arrhenius plot, could be indicative of a parallel mechanism involving the stepwise pathway as a secondary channel. Under such conditions, the measured reaction rate would amount to the sum of two competing reaction channels, and the measured Arrhenius parameters would show significant deviation from the estimates provided above.

4. Conclusions

Characterization of the potential surface of acetylene ozonation in this study provides the first theoretical evidence for a biradical stepwise pathway. In contrast to the previous theoretical study, the stepwise pathway can be recovered by both single- and multireference methods. Comparison between the two methods for their estimates of the energy of concert highlights a central difficulty in the characterization of a PES exhibiting discontinuity originating from the wave function instability in the concerted pathway transition state and O_3. With the multireference approach, there is only one estimate of E_c, whereas using the CCSD(T)//DFT approach, different values are obtained depending on the choice of the use of the spin-restricted or spin-unrestricted methods on the partial biradical structures in the PES. E_c derived from the comparison between two separate PESs predicts the concerted pathway as the only significant reaction mechanism. E_c derived from a single, continuous, global PES suggests a parallel pathway mechanism wherein the stepwise pathway competes with the concerted pathway as a secondary channel at elevated temperatures. The notion of a parallel mechanism provides one possible explanation of the observation of a high-entropy transition state reported nearly four decades ago.

A detailed analysis has been provided for future experimental investigations to verify the mechanism. Arrhenius parameters predicted for the concerted pathway are expected to be of sufficient accuracy for the identification of a concerted mechanism. Non-Arrhenius kinetic behavior as a possible experimental indication of a parallel mechanism is suggested. Multitemperature measurements are suggested for the detection of such a mechanism.

As this report was being brought to completion, we were informed of a very recent study on the kinetics of acetylene ozonation. It was reported by Du et al.[34] that measurements at 288 K yield a rate constant of 4.13×10^{-21}cm^3 molecule^{-1} s^{-1}. The deviation between this value and DeMore's Arrhenius plot is consistent with the discrepancy between DeMore's $k(T)$ (1971) and that of Aschmann and Atkinson.[35] Acceptance of this result does not invalidate the analysis reported herein. However, it is supportive of the assumption that the lowest $k(T)$ is the most accurate and raises the possibility that the real room-temperature rate constant could fall below the lower limit of known experimental data. Hence, this suggests that observation of a low A factor associated with the concerted pathway is the more likely outcome.

Acknowledgment. Financial support for this research provided by the Natural Science and Engineering Research Council of Canada to J.D.G. is gratefully acknowledged. The provision of computer resources by Sharcnet also is acknowledged.

Supporting Information Available: Cartesian coordinates for all stationary points. This material is available free of charge via the Internet at http://pubs.acs.org.

References and Notes

(1) Atkinson, R.; Carter, W. P. L. *Chem. Rev.* **1984**, *84*, 437.
(2) Cadle, R. D.; Schadt, C. *J. Chem. Phys.* **1953**, *21*, 163.
(3) DeMore, W. B. *Int. J. Chem. Kinet.* **1969**, *1*, 209.
(4) DeMore, W. B. *Int. J. Chem. Kinet.* **1971**, *3*, 161.
(5) Stedman, D. H.; Niki, H. *Environ. Lett.* **1973**, *4*, 303.
(6) Pate, C. T.; Atkinson, R.; Pitts, J. N., Jr. *J. Environ. Sci. Health, Part A* **1976**, *11*, 1.
(7) Atkinson, R.; Aschmann, S. M. *Int. J. Chem. Kinet.* **1984**, *16*, 259.
(8) Sander, S. P.; Golden, D. M.; Kurylo, M. J.; Moortgat, G. K.; Ravishankara, A. R.; Kolb, C. E.; Molina, M. J.; Finlayson, B. J. *Chemical Kinetics and Photochemical Data for Use in Atmospheric Studies*; Jet Propulsion Laboratory Publication 02-25, Evaluation Number 14; Pasadena, CA, 2003, Note D6.
(9) Atkinson, R.; Baulch, D. L.; Cox, R. A.; Crowley, J. N.; Hampson, R. F., Jr.; Hynes, R. G.; Jenkin, M. E.; Kerr, J. A.; Rossi, M. J.; Troe, J. *Summary of Evaluated Kinetic and Photochemical Data for Atmospheric Chemistry*; Chemical Kinetics Data Center, National Institute of Standards and Technology: Gaithersburg, Maryland, 2006.
(10) (a) Cremer, D.; Kraka, E.; Crehuet, R.; Anglada, J.; Grafenstein, J. *Chem. Phys. Lett.* **2001**, *347*, 268. (b) Ref 10a reports a calculated value of 0.13 units (quoted as 0.8 M^{-1} s^{-1}) for k_{298} compared with the NASA value of 1 unit. A k_{298} of 48.3 M^{-1} s^{-1} is attributed to DeMore's study. DeMore's 1969 study, referred to in ref 10a, was carried out in a temperature range from 243 to 283 K, and no room temperature measurement was reported. The measured rate constants fall in the range of 0.3−11.8 M^{-1} s^{-1}. DeMore's rate constant measured at 294 K reported in the 1971 study (18 M^{-1} s^{-1}) is, in fact, in closer agreement with the NASA-recommended value than the calculated value of ref 10a. (c) Ref 10a reports an A factor of 1.71×10^6 M^{-1} s^{-1} calculated with transition state theory (TST) at 298 K, which is in close agreement with the recommended value in the NASA database. However, a uniquely defined A factor cannot be derived for only one single temperature with TST. Experimental Arrhenius parameters are obtained from multitemperature kinetic measurements. An A factor calculated for a single temperature with TST can assume two different values, depending on the choice of the reference energy level in the evaluation of the total vibrational partition function. (d) The barrier heights quoted in the discussion in ref 10a are 10.5 kcal/mol, which is the CCSD(T) room-temperature activation enthalpy ($\Delta H^{\ddagger}_{298}$), and the CCSD(T)/CBS values of 9.6 kcal/mol. These values are referenced to the energy level of the vdW complex of the reactants. Adjustment of the reference energy level to HCCH + O_3 gives a CCSD(T) value of 8.11 kcal/mol for $\Delta E^{\ddagger}$ and 9.53 kcal/mol for $\Delta H^{\ddagger}_0$ and CCSD(T)/CBS values of 7.09 and 8.51 kcal/mol for $\Delta E^{\ddagger}$ and $\Delta H^{\ddagger}_0$, respectively. The zero-point energies used for evaluation of energy changes in ref 10a were calculated with DFT-B3LYP (with the exception of the vdW complex). Geometry optimizations were carried out at the CCSD(T) level.
(11) Houk, K. N.; Gonzalez, J.; Li, Y. *Acc. Chem. Res.* **1995**, *28*, 81.
(12) Wiest, O.; Montiel, D. C.; Houk, K. N. *J. Phys. Chem. A* **1997**, *101*, 8378.
(13) (a) Chan, W.-T.; Hamilton, I. P. *J. Chem. Phys.* **2003**, *118*, 1688. (b) In ref 13a, BHandHLYP/6-31+G(d) was employed for the A factor calculations for $T = 235-362$ K. The value of log A (A in mole^{-1} cm^3 s^{-1}) obtained for the concerted pathway of the ozonation of ethylene is 9.96, compared with the experimental value[28] of 9.73. For propene, the calculated value is 9.40, compared with the experimental value of 9.57.
(14) Yoshioka, Y.; Tsunesada, T.; Yamaguchi, K.; Saito, I. *Int. J. Quantum Chem.* **1997**, *65*, 787.
(15) Cremer, D.; Crehuet, R.; Anglada, J. *J. Am. Chem. Soc.* **2001**, *123*, 6127.
(16) Fukutome, H. *Int. J. Quantum Chem.* **1981**, *20*, 955.
(17) Bartlett, R. J. *Int. J. Mol. Sci.* **2002**, *3*, 579.
(18) Freccero, M.; Gandolfi, R.; Sarzi-Amade, M.; Rastelli, A. *J. Org. Chem.* **2003**, *68*, 811.
(19) Grafenstein, J.; Hjerpe, A. M.; Kraka, E.; Cremer, D. *J. Phys. Chem. A* **2000**, *104*, 1748.
(20) Frisch, M. J.; Trucks, G. W.; Schlegel, H. B.; Scuseria, G. E.; Robb, M. A.; Cheeseman, J. R.; Zakrzewski, V. G.; Montgomery, J. A., Jr.; Stratmann, R. E.; Burant, J. C.; Dapprich, S.; Millam, J. M.; Daniels, A. D.; Kudin, K. N.; Strain, M. C.; Farkas, O.; Tomasi, J.; Barone, V.; Cossi, M.; Cammi, R.; Mennucci, B.; Pomelli, C.; Adamo, C.; Clifford, S.; Ochterski, J.; Petersson, G. A.; Ayala, P. Y.; Cui, Q.; Morokuma, K.; Malick, D. K.; Rabuck, A. D.; Raghavachari, K.; Foresman, J. B.; Cioslowski, J.; Ortiz, J. V.; Stefanov, B. B.; Liu, G.; Liashenko, A.; Piskorz, P.; Komaromi, I.; Gomperts, R.; Martin, R. L.; Fox, D. J.; Keith, T.; Al-Laham, M. A.; Peng, C. Y.; Nanayakkara, A.; Gonzalez, C.; Challacombe, M.; Gill, P. M. W.; Johnson, B. G.; Chen, W.; Wong, M. W.; Andres, J. L.; Head-Gordon, M.; Replogle, E. S.; Pople, J. A. *Gaussian 98*, revision A.11; Gaussian, Inc.: Pittsburgh, PA, 1998.
(21) Frisch, M. J.; Trucks, G. W.; Schlegel, H. B.; Scuseria, G. E.; Robb, M. A.; Cheeseman, J. R.; Montgomery, J. A., Jr.; Vreven, T.; Kudin, K. N.; Burant, J. C.; Millam, J. M.; Iyengar, S. S.; Tomasi, J.; Barone, V.; Mennucci, B.; Cossi, M.; Scalmani, G.; Rega, N.; Petersson, G. A.; Nakatsuji, H.; Hada, M.; Ehara, M.; Toyota, K.; Fukuda, R.; Hasegawa, J.; Ishida, M.; Nakajima, T.; Honda, Y.; Kitao, O.; Nakai, H.; Klene, M.; Li, X.; Knox, J. E.; Hratchian, H. P.; Cross, J. B.; Bakken, V.; Adamo, C.; Jaramillo, J.; Gomperts, R.; Stratmann, R. E.; Yazyev, O.; Austin, A. J.; Cammi, R.; Pomelli, C.; Ochterski, J. W.; Ayala, P. Y.; Morokuma, K.; Voth, G. A.; Salvador, P.; Dannenberg, J. J.; Zakrzewski, V. G.; Dapprich, S.; Daniels, A. D.; Strain, M. C.; Farkas, O.; Malick, D. K.; Rabuck, A. D.; Raghavachari, K.; Foresman, J. B.; Ortiz, J. V.; Cui, Q.; Baboul, A. G.; Clifford, S.; Cioslowski, J.; Stefanov, B. B.; Liu, G.; Liashenko, A.; Piskorz, P.; Komaromi, I.; Martin, R. L.; Fox, D. J.; Keith, T.; Al-Laham, M. A.; Peng, C. Y.; Nanayakkara, A.; Challacombe, M.; Gill, P. M. W.;

Johnson, B.; Chen, W.; Wong, M. W.; Gonzalez, C.; Pople, J. A. *Gaussian 03*, revision D.01; Gaussian, Inc.: Wallingford, CT, 2004.
(22) Schmidt, M. W.; Baldridge, K. K.; Boatz, J. A.; Elbert, S. T.; Gordon, M. S.; Jensen, J. H.; Koseki, S.; Matsunaga, N.; Nguyen, K. A.; Su, S. J.; Windus, T. L.; Dupuis, M.; Montgomery J. A. *J. Comput. Chem.* **1993**, *14*, 1347.
(23) Pulay, P.; Hamilton, T. P. *J. Chem. Phys.* **1987**, *88*, 4926.
(24) Borden, W. T.; Davidson, E. R. *Acc. Chem. Res.* **1996**, *29*, 67.
(25) Jensen, F. *J. Am. Chem. Soc.* **1989**, *111*, 367.
(26) Nakano, H. *J. Chem. Phys.* **1993**, *99*, 7983.
(27) Glaesemann, K. R.; Gordon, M. S.; Nakano, H. *Phys. Chem. Chem. Phys.* **1999**, *1*, 967.
(28) Herron, J. T.; Huie, R. E. *J. Phys. Chem.* **1974**, *78*, 2085.
(29) Zaman, M. H.; Sosnick, T. R.; Berry, R. S. *Phys. Chem. Chem. Phys.* **2003**, *5*, 2589.
(30) Ayala, P. Y.; Schelgel, H. B. *J. Chem. Phys.* **1998**, *108*, 2314.
(31) Barone, V. *J. Chem. Phys.* **2004**, *120*, 3059.
(32) Truhlar, D. G.; Isaacson, A. D. *J. Chem. Phys.* **1991**, *94*, 357.
(33) Sinnokrot, M. O.; Sherill, C. D. *J. Chem. Phys.* **2001**, *115*, 2439.
(34) Du, L.; Xu, Y.-F.; Ge, M.-F.; Jia, L.; Wang, G.-C.; Wang, D.-X. *Acta Chim. Sin.* **2006**, *64*, 2133.
(35) Fitting of this $k(T)$ to DeMore's Arrhenius plot requires a correction of of the A factor to log $A = 8.6$ or E_a to 12 kcal/mol.